Eph tyrosine kinase receptor EphA4 is required for the topographic mapping of the corticospinal tract

Alison J. Canty*†, Ursula Greferath*, Ann M. Turnley‡, and Mark Murphy*§

*Department of Anatomy and Cell Biology and ‡Centre for Neuroscience, University of Melbourne, Victoria 3010, Australia

Communicated by Gustav J. Nossal, University of Melbourne, Victoria, Australia, August 24, 2006 (received for review October 18, 2005)

Fine movement in the body is controlled by the motor cortex, which signals in a topographically specific manner to neurons in the spinal cord by means of the corticospinal tract (CST). How the correct topography of the CST is established is unknown. To investigate the possibility that the Eph tyrosine kinase receptor EphA4 is involved in this process, we have traced CST axons in mice in which the EphA4 gene has been deleted. The forelimb subpopulation of CST axons is unaffected in the *EphA4*$^{-/-}$ mice, but the hindlimb subpopulation branches too early within the cord, both temporally and spatially. EphA4 shows a dynamic expression pattern in the environment of the developing CST in the spinal cord: high at the time of forelimb branching and down-regulated before hindlimb branching. To examine whether the fore- and hindlimb subpopulations of CST axons respond differently to EphA4 in their environment, neurons from fore- and hindlimb motor cortex were cultured on a substrate containing EphA4. Neurons from the hindlimb cortex showed reduced branching on the EphA4 substrate compared with their forelimb counterparts. Neurons from the hindlimb cortex express ephrinA5, a high-affinity ligand for EphA4, at higher levels compared with forelimb cortex neurons, and this expression is down-regulated before hindlimb branching. Together, these findings suggest that EphA4 regulates topographic mapping of the CST by controlling the branching of CST axons in the spinal cord.

motor control | axon guidance | spinal cord | neuronal development

Fine voluntary movement is controlled by the motor areas of the cerebral cortex. The motor cortex has a somatotopic arrangement in which different areas control movements of different parts of the body. For those regions of the motor cortex that control movement of the muscles of the trunk and limbs, the cortical commands travel through the brain in the corticospinal tract (CST) to terminate in topographically specific locations along the spinal cord. There are two major termination zones in the spinal cord, in the cervical and lumbar regions, that carry information for the fore- and hindlimbs, respectively. In primates, the CST axons terminate directly on spinal motor neurons and interneurons, whereas in other mammals, termination occurs almost exclusively on interneurons in the dorsal horns. The CST thus provides the most direct route for cortical control of movement and is the longest and largest descending tract from the brain.

During development, growing CST axons must navigate long distances through the brain and spinal cord to reach their gray-matter target cells. How they are successfully guided to their target locations in a topographically correct pattern is unknown. In rodents, CST axons descend through the spinal cord in the ventral aspect of the dorsal funiculus (DF). The axons then exit the DF in topographically specific locations along the cord by means of collateral branching. Several *in vivo* and *in vitro* explant studies suggest that as-yet-unidentified diffusible and/or contact-mediated cues may be involved in regulating this event (1–4).

The Eph receptors and their ephrin ligands have been implicated in topographical mapping of developing circuitry (5). We and others have shown that one of these receptors, EphA4, is required for development of the CST (6–8). EphA4-null mutants have a striking hopping gait (7), resulting from disruption of local neuronal circuits that control walking (9). In the CST, there are major disruptions in the spinal cord, including inappropriate midline crossing, an increase in CST axons in the gray matter in cervical regions, and a decrease of CST axons in lumbar regions in adult mice (6–8). The mode of action of EphA4 in preventing CST axons from recrossing the midline has been examined (6, 10), but our findings suggest that EphA4 is involved in a number of guidance decisions for CST axons in the spinal cord, including guiding the CST down and/or laterally within the spinal cord. Here, we provide evidence that EphA4 regulates the topographic organization of the CST by controlling the time and place of branching of subpopulations of CST axons into the gray matter of the spinal cord.

Results

Loss of Topographically Specific Branching of CST Axons in Spinal Cords of EphA4 Mutant Mice. We investigated the possibility that EphA4 is involved in guiding the CST down and/or laterally within the spinal cord. To do this, we have undertaken quantitative anterograde tracing of the CST in *EphA4*$^{-/-}$ mice at the time of its descent and collateral branching in the spinal cord (Fig. 5, which is published as supporting information on the PNAS web site). Biotinylated dextran amine (BDA) was injected into the anterior cortex of *EphA4*$^{-/-}$ and control mice at postnatal day (P)1, and spinal cords were examined at both P5 and P7, which spans the time of collateral branching of CST axons in the cervical spinal cord (11). Branches from the axon shaft are present at these times (Fig. 5); later in development, it is difficult to identify branches because the axon shafts within the DF degenerate back to their branch points (12).

A number of possibilities could explain the increase of CST axons in the cervical spinal cord in the *EphA4*$^{-/-}$ mice. First, EphA4 interactions may be involved in guiding the CST axons down the descending tract (ventral DF) in the spinal cord. In the absence of EphA4, CST axons may lose this guidance, no longer be contained within the DF, and grow directly out of it without branching. We examined this possibility by determining the number of axons that exited directly out of the DF without branching. In all animals, only a very small number of axons exited the DF in the cervical spinal cord without branching (0.6%), and there was no difference between control ($n = 5$ at P5; $n = 6$ at P7) and *EphA4*$^{-/-}$ ($n = 5$ at P5; $n = 8$ at P7) mice. Thus, these findings do not provide evidence that EphA4 is involved in guiding the CST axons down the DF.

A second possibility is that EphA4 regulates the frequency of

Author contributions: A.J.C., U.G., A.M.T., and M.M. designed research; A.J.C. and U.G. performed research; A.J.C. and M.M. analyzed data; and A.J.C. and M.M. wrote the paper.

The authors declare no conflict of interest.

Abbreviations: BDA, biotinylated dextran amine; CST, corticospinal tract; DF, dorsal funiculus; PSA-NCAM, polysialated neural cell adhesion molecule; P*n*, postnatal day *n*.

†Present address: Division of Molecular Neurobiology, Department of Neuroscience, Karolinska Institute, S-171 77 Stockholm, Sweden.

§To whom correspondence should be addressed. E-mail: m.murphy@unimelb.edu.au.

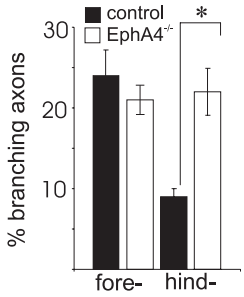

Fig. 1. Topographic mapping of the CST is disrupted in *EphA4*$^{-/-}$ mice. To investigate whether fore- and hindlimb CST axons behaved differently in *EphA4*$^{-/-}$ mice compared with control mice, they were separately labeled with the anterograde tracer BDA. The percentage of fore- and hindlimb axons that branched into the gray matter of the cord was measured in mutant and control mice. Significantly more hindlimb axons branched into the gray matter in *EphA4*$^{-/-}$ mice compared with control mice. *, $P < 0.01$.

branching of each axon into the gray matter, where loss of EphA4 results in an increase in the number of branches per axon. However, in both control and *EphA4*$^{-/-}$ animals, the frequency of branches per axon was identical (1.0 ± 0.02, $n = 373$ axons for *EphA4*$^{-/-}$ mice, $n = 405$ axons for control mice). This result suggests that EphA4 does not regulate the number of branches per axon that enter the gray matter in the cervical spinal cord.

The third possibility is that EphA4 is involved in the topographically specific exit of CST axons along the spinal cord. If true, there might be topographically inappropriate branching of hindlimb axons out of the DF in the cervical region of *EphA4*$^{-/-}$ mice. To examine this possibility, BDA was injected into the rostral and caudal regions of the motor cortex in separate mice (Fig. 5). Forelimb corticospinal neurons are found predominantly in rostral regions of the motor cortex, whereas the hindlimb population are mainly found in caudal regions (13, 14). The precise location of the injections was confirmed before analysis of each cervical spinal cord (Fig. 5), and those brains with injections outside the specified coordinates were excluded. Our previous tracing studies of the CST in *EphA4*$^{-/-}$ mice showed that the motor cortex is not displaced in the these mice (8), making injections into the different regions of the control and *EphA4*$^{-/-}$ motor cortex comparable.

In mice that were injected in the rostral cortex, there was no difference between control ($n = 5$) and *EphA4*$^{-/-}$ ($n = 5$) mice in the proportion of axons that branched into the cervical cord (Fig. 1), suggesting that forelimb branching is unaffected by the absence of EphA4. In contrast, in mice that were injected in the caudal motor cortex, there were significant differences between control and *EphA4*$^{-/-}$ mice. In control mice ($n = 6$), a low but significant percentage of caudally derived CST axons branched in cervical regions of the spinal cord (Fig. 1). In contrast, in *EphA4*$^{-/-}$ mice ($n = 8$), a significantly higher proportion of labeled axons ($P < 0.01$) branched at the cervical level. The proportion of caudally derived CST axons that showed inappropriate branching in the *EphA4*$^{-/-}$ mice was in the same range as the proportion of axons that showed topographically correct branching from rostral regions of the cortex. Thus, these findings show a major disruption in topographic targeting of the CST in *EphA4*$^{-/-}$ mice, with the hindlimb axons branching too early, both spatially (cervical instead of lumbar) and temporally [by P7 instead of from P10 (11)].

It was still possible that EphA4 is required for guidance of CST axons down the cord and that the ectopic branching of the hindlimb axons is secondary and resultant from defective descent of these axons below the cervical region in the *EphA4*$^{-/-}$ mice. To examine this possibility, we counted the number of labeled hindlimb axons that had reached the lumbar cord at P7 and expressed this number as a percentage of labeled axons in the cervical cord in the same animal; P7 is a time when CST axons have reached the lumbar cord but degeneration of the primary axon shaft has not yet occurred (11, 12). A similar percentage of axons had reached the lumbar cord at P7 in both *EphA4*$^{-/-}$ mice ($84 \pm 12\%$, $n = 3$) and their heterozygous littermates ($88 \pm 16\%$, $n = 4$), which is consistent with our findings described above that EphA4 is not involved in guiding CST axons down the spinal cord. We could not detect any branching of these axons in the lumbar cord in *EphA4*$^{-/-}$ mice or controls.

EphA4 Expression Decreases in the Spinal Cord at the Time of Branching of Hindlimb CST Axons. Previous studies suggest that complementary gradients of Eph receptors and their ligands in projection and target fields are involved in topographic mapping within the nervous system (5). If a similar mechanism operates for the CST, EphA4 may be differentially expressed within CST axons or in their environment in the DF. To examine these possibilities, we analyzed EphA4 expression in the developing neonatal spinal cord. By P5, the majority of axons have arrived in the cervical spinal cord, and the forelimb axons have commenced collateral branching into the gray matter (11). In the cervical DF at this age, there is strong EphA4 expression, particularly in the most ventral region, which contains the growing CST axons (Fig. 6, which is published as supporting information on the PNAS web site). However, EphA4 also appeared to be expressed outside the CST, which is confined to the ventromedial aspect of the DF (15). Furthermore, EphA4 was strongly expressed in the ventral DF before the arrival of any CST axons (11): in cervical and lumbar regions of the cord at P0 and in the lumbar cord at P5 (Fig. 6). Thus, EphA4 may be expressed both on CST axons and in their environment in the DF. Expression of EphA4 was maintained in the DF until at least P11, when the CST has reached the lumbar cord (Fig. 6).

To show expression on CST axons, we labeled the axons with BDA as described above and double-labeled them with EphA4. Some of the EphA4 expression colocalized with BDA-labeled projections from the anterior cortex (Fig. 6), consistent with a previous report of EphA4 expression on CST axons (16). We then examined whether EphA4 was differentially expressed within the CST. Because of the dense labeling of EphA4 across the DF and the fact that fore- and hindlimb CST axons are tightly fasciculated with each other, it was difficult to determine whether they express different levels of EphA4 within the DF. To determine whether there was any differential expression in these subpopulations, we examined EphA4 expression in the motor neurons in layer 5 of the fore- and hindlimb motor cortex. Expression across layer 5 is evident from birth, persists until at least P11 (data not shown), and is highest at P5; however, there is no observable difference in expression between the rostral (forelimb) and caudal (hindlimb projection) regions at this age (Fig. 6). Further, pixel density measurements show no significant difference in EphA4 immunoreactivity between these regions of the motor cortex (forelimb, 0.149 ± 0.017; hindlimb, 0.155 ± 0.016).

We then examined EphA4 expression within the DF more closely by labeling sections with a polysialated neural cell adhesion molecule (PSA-NCAM) antibody, which is expressed by the great majority of CST axons as they descend through the spinal cord (17, 18), as well as other axons within the gray matter of the cord. This labeling allowed us to distinguish CST from environmental (non-CST) EphA4 expression in the neonatal DF. Immunolabeling of sections of P5 cervical spinal cord for PSA-NCAM (red) showed clear immunoreactivity in the ventromedial DF, confirming the location of the CST (Fig. 2*a*). Labeling the same sections for EphA4 (green) showed expression that overlapped with the PSA-NCAM^{+} CST axons and

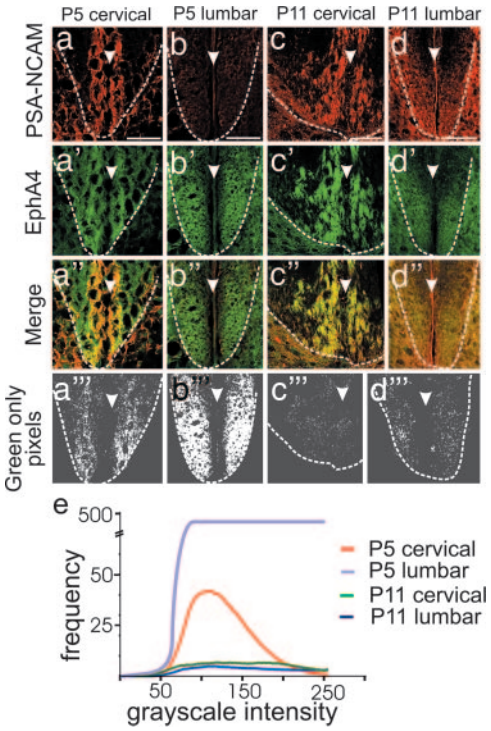

Fig. 2. Expression of EphA4 in the environment of the CST axons decreases in the DF between P5 and P11. (*a*–*d*‴) Sections of the ventral DF at P5 cervical (*a*) and lumbar (*b*) and P11 cervical (*c*) and lumbar (*d*) levels are shown. *a*–*d* show PSA-NCAM expression in red, which identifies CST axons. *a*′–*d*′ show EphA4 expression in green. *a*″–*d*″ show merged images of PSA-NCAM and EphA4 labeling with regions of overlap in yellow. An imaging program (AnalySIS) was used to select the green-only pixels from the merged images (*a*‴–*d*‴), shown in white. Dotted lines in *a*–*d*‴ indicate the ventral boundary of the DF. Arrowheads indicate the midline of the spinal cord. (Scale bars, which apply to *a*–*d*‴: 100 μm.) (e) The frequency and intensity of green-only pixels in *a*‴–*d*‴ were quantitated and are shown as a histogram. The intensity of green-only pixels in the P5 lumbar cord was 10-fold higher, and the scale of the *y* axis has been adjusted accordingly.

surrounded them (Fig. 2 *a* and *a*″). At P5, there was significant expression of environmental EphA4 in the cervical DF (Fig. 2 *a*′ and *a*″); in the lumbar DF at P5, before arrival of the CST, EphA4 is strongly expressed and exclusively environmental (Fig. 2 *b* and *b*″).

At P11, the CST has innervated the lumbar enlargement of the cord, where it is more loosely fasciculated and is undergoing branching (11). EphA4 immunoreactivity at this age was still strong (Fig. 2 *c*′ and *d*′) but was mostly colocalized with PSA-NCAM (Fig. 2 *c*, *c*″, *d*, and *d*″), indicating that environmental expression of EphA4 has decreased at this age. The relative levels of nonaxonal EphA4 immunoreactivity at P5 and P11 in cervical and lumbar regions of the spinal cord were quantitated by isolating all remaining green pixels in the merged images of EphA4–PSA-NCAM immunoreactivity (Fig. 2 *a*‴–*d*‴). In the cervical DF at P5, environmental expression of EphA4 was significantly higher than in the lumbar DF at P11 (Fig. 2*e*; $P = 0.011$).

This profile of EphA4 expression, combined with our tracing studies, suggests how EphA4 might regulate topographic mapping of the CST. The tracing studies show that targeting and branching of hindlimb CST axons is disrupted in *EphA4*$^{-/-}$ mice, indicating that EphA4 regulates the exit of the hindlimb CST axons from the DF. Within the DF, EphA4 is expressed both on CST axons and in their surrounding environment, but expression seems to change only in the environment and is high at the time

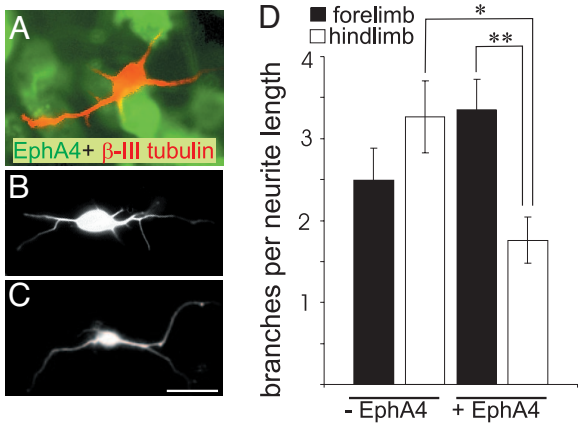

Fig. 3. Postnatal fore- and hindlimb cortical neurons respond differently when grown on a substrate containing EphA4. Cortical neurons were cultured on monolayers of 293T cells transfected with EphA4 or control plasmids and visualized with B-III tubulin; EphA4 expression was identified with immunostaining. (*A*) A β-III tubulin neuron (red) on EphA4-expressing cells (green). (*B* and *C*) Representative neurons from P3 fore- and hindlimb motor cortex, respectively. (Scale bar: 10 μm.) (*D*) The frequency of branches per 100 μm of primary neurite length for these neurons under each condition. *, $P = 0.02$; **, $P = 0.006$. Error bars indicate SEM.

of forelimb branching and low at the time of hindlimb branching. Thus, the level of EphA4 in the environment may control when and where the hindlimb CST axons branch in the cord, which would explain why hindlimb axons exit in the cervical cord in the absence of EphA4.

***In Vitro* Analysis of Fore- and Hindlimb Populations Grown on an EphA4 Substrate.** Previous *in vitro* studies show that embryonic cortical neurites expressing EphA4 are able to respond to an ephrin ligand environment, resulting in growth cone collapse (10). However, we recently found that when embryonic cortical neurons were grown on a substrate of EphA4 expressing 293T cells, they extended shorter neurites than when grown on control 293T cells, indicating that neurite outgrowth is inhibited by EphA4 (19). To investigate whether neurons within different regions of the motor cortex can respond differentially to an EphA4 substrate, we conducted neurite outgrowth assays using cortical neurons from postnatal fore- and hindlimb motor cortex. The middle lamellae of P3 fore- and hindlimb cortex, which contains a large proportion of layer 5 cells (Fig. 7, which is published as supporting information on the PNAS web site), was dissociated and added to a confluent layer of 293T cells expressing EphA4. After 24 h in culture, the neurons had commenced branching. The hindlimb neurons showed significantly less branching ($P = 0.02$) on the EphA4 substrate compared with the control substrate (Fig. 3). In comparison, there was no significant difference in branching of forelimb neurons in the presence or absence of EphA4 (Fig. 3). The hindlimb neurons also showed significantly less branching ($P = 0.006$) on the EphA4 substrate compared with forelimb neurons (Fig. 3). These differences in branching are consistent with the *in vivo* behavior of these subpopulations in the spinal cord. The forelimb axons undergo collateral branching in an EphA4^{+} environment, whereas the hindlimb axons do not branch until EphA4 in the environment is down-regulated, or they branch inappropriately in the cervical cord in the absence of EphA4 in the *EphA4*$^{-/-}$ mice.

EphrinA5 Is Differentially Expressed Within Subpopulations of Neurons in the Motor Cortex and on the CST. To look for potential ephrin ligands that might interact with EphA4 in the DF, we examined spinal cord sections at P5 and P11 by using a number

NEUROSCIENCE

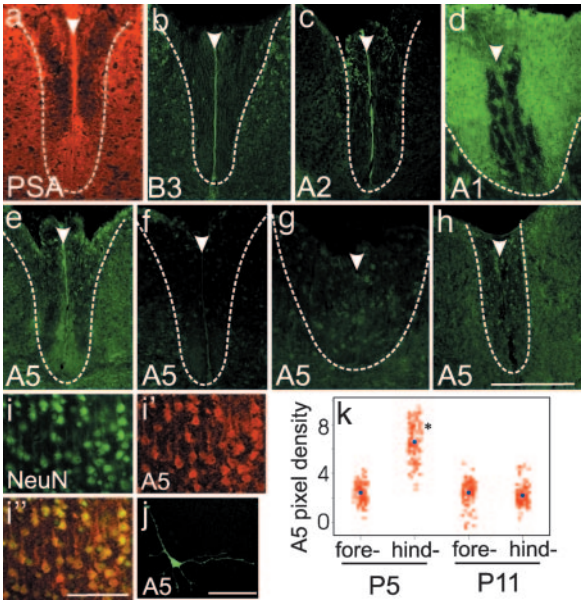

Fig. 4. Ephrin expression in the postnatal spinal cord and cortex. (*a–h*) Expression in the spinal cord of PSA-NCAM (*a*, red) and ephrins (*b–h*, green). (*a*) PSA-NCAM profile in the DF at P5 indicates the location of CST in the ventral region. (*b* and *c*) EphrinB3 (*b*) and -A2 (*c*) are expressed along the midline of the DF at P0 and P2, respectively. (*d*) EphrinA1 is highly expressed in the dorsal and lateral regions of the DF at P11. (*e*) EphrinA5 expression is present in the ventromedial region of the DF in the P5 cervical spinal cord and matches the profile of the PSA-NCAM$^+$ CST (shown in *a*). (*f–h*) There is no significant ephrinA5 expression in the ventral DF in lumbar levels at either P5 (*f*) or P11 (*h*) or in the P11 cervical DF (*g*). Dotted lines in *a–h* indicate the boundary of the DF. Arrowheads indicate the midline of the spinal cord. (*i–i″*) Expression of NeuN (*i*, green) and ephrinA5 (*i′*, red) in layer 5 of the hindlimb motor cortex at P5. *i″* shows a merge of NeuN and ephrinA5 labeling. (*j*) Cultured hindlimb cortical neuron labeled for ephrinA5 (green) shows immunoreactivity on processes. (Scale bars: *a–f*, *i*, and *j*, 50 μm; *g* and *h*, 100 μm.) (*k*) Distribution of ephrinA5 immunoreactivity in layer 5 neurons in fore- and hindlimb motor cortex at P5 and P11. The mean intensity (optical density $\times 10^{-2}$, blue dots) in the P5 hindlimb motor cortex is significantly higher than in all other conditions. *, $P = 0.0005$.

of ephrin antibodies. More specifically, we were looking for expression within, or immediately surrounding, the developing CST (Fig. 4*a*). EphA4 has high affinity with ephrinA5, -A1, -A2, and -A6 and has clear functional interaction with ephrinB3 during the development of the CST (10, 20, 21). We examined the expression of each of these ephrins in the postnatal DF, with the exception of ephrinA6, which is not present in mice (http://mouseblast.informatics.jax.org/). All of these ephrins were expressed in the DF. Both ephrinB3 and -A2 were expressed along the midline of the spinal cord, including the DF, and at the highest levels approximately from birth to P2 (Fig. 4 *b* and *c*). EphrinA1 was also expressed in the DF, but the pattern of expression was concentrated in dorsal regions, where it became strongly expressed in the dorsal white matter from P9 (Fig. 4*d*).

The only ligand we found that was expressed in the region of the CST was ephrinA5, which was localized to the cervical DF at P5 (Fig. 4*e*). The pattern of immunolocalization within the DF matched that seen with PSA-NCAM (Fig. 4*a*), consistent with expression of ephrinA5 on the CST axons. Expression was very low or undetectable in the cervical DF at P11 (Fig. 4*g*) and was not detected in the lumbar DF at any age (Fig. 4 *f* and *h*). This result suggests that expression of ephrinA5 is down-regulated by P11. We also probed sections with an EphA4–Fc fusion protein, which is capable of detecting any ligand to which EphA4 is able to bind (22, 23). Binding of EphA4–Fc to spinal cord sections did not reveal any further possible ligand expression above what was already described (data not shown).

To determine whether different subpopulations of cortical motor neurons express ephrinA5, we investigated expression in the developing motor cortex. EphrinA5 labeling is evident in the fore- and hindlimb motor cortex at P5 and P11 (Fig. 4 *i* and *k*), at the time of collateral branching in the cervical and lumbar enlargements, respectively. Within layer 5, at both ages, the majority of labeled cells colocalized with pyramidal cells that were immunoreactive for the neuronal marker NeuN (89 ± 3%, $n = 6$; Fig. 4 *i–i″*), indicating that ephrinA5 is expressed by the pyramidal cortical neurons. These neurons also expressed ephrinA5 in culture and showed clear expression on processes (Fig. 4*j*), consistent with their axonal expression in the spinal cord. Two distinct trends in ephrinA5 expression were observed. First, at P5, ephrinA5 immunoreactivity was markedly stronger in the hindlimb motor cortex compared with the forelimb cortex. Second, there was a decrease in ephrinA5 expression within the hindlimb motor cortex, from higher levels at P5 to much lower levels at P11. This trend was reflected in the mean pixel density of ephrinA5 immunoreactivity in these populations, which was 2.9-fold higher in the P5 hindlimb compared with the P5 forelimb cortex and the entire motor cortex at P11 (Fig. 4*k*; $P = 0.0005$).

The differential expression of ephrinA5 in motor cortex and cervical CST can be correlated with the topographically specific branching of different CST axons within the spinal cord. Our data suggest that, at P5, forelimb axons expressing low levels of ephrinA5 branch and exit the DF, whereas hindlimb axons expressing higher levels of ephrinA5 continue to descend through the DF. By P11, ephrinA5 expression has decreased in the hindlimb axons, at which time this population exits in the lumbar cord.

Discussion

Our results show that there is major disruption in topographically specific targeting and branching of the CST in the *EphA4*$^{-/-}$ mice. Whereas the forelimb axons exit normally, the hindlimb populations branch and exit too early, both temporally and spatially, into the cervical spinal cord. These results suggest that EphA4 regulates topographic mapping of the CST by preventing branching of the hindlimb subpopulation of axons at the incorrect time and location (see Fig. 8, which is published as supporting information on the PNAS web site, for scheme).

Our data also show that early during development of the CST, the growth of the hindlimb axons down the spinal cord is not affected in the *EphA4*$^{-/-}$ mice, and very few axons simply turn out of the DF without branching. These results suggest that EphA4 does not play a significant role in guiding the CST axons in their descent through the DF. Our findings are consistent with the findings of others that showed that descent through the DF and topographically specific branching are discrete events in CST guidance (1, 4, 24). Recent data suggest that members of the Wnt family are involved in guiding CST axons down the cord (25). By adulthood, only low numbers of CST axons were found in the lumbar cord of the *EphA4*$^{-/-}$ mice (7), probably because many of the hindlimb axon shafts had degenerated back to their ectopic branch points in the cervical cord.

During development, EphA4 is expressed both on the CST axons and in the environment surrounding them. We could not find any evidence for differential expression between fore- and hindlimb subpopulations of the CST, but EphA4 is down-regulated in the environment at the time the hindlimb axons exit. EphA4 within the environment of the developing CST may thus prevent branching of the hindlimb axons at the incorrect time and place (Fig. 8). Our *in vitro* assays support a role for EphA4 in the environment by distinguishing forelimb axons from hindlimb axons. These two major subpopulations of CST axons respond differently to an environment containing EphA4, with

neurons from the hindlimb motor cortex showing significantly less neurite branching compared with neurons from forelimb motor cortex. The EphA4 in the environment may be expressed by interweaving processes of glial cells (26–28), which are present in the DF during CST development. These glia first appear at approximately embryonic day 15 (29), close to the time when we first detect EphA4 in this region (30). Glial EphA4 may have a related role in the adult. Our recent data show that, after spinal cord injury, EphA4 is expressed on glia, inhibiting the growth of several axonal pathways, including the CST, and regulating astrocytic gliosis (19).

Eph receptor signaling can mediate both repulsion (20) and adhesion/fasciculation (31–33). In the case of topographical mapping of the CST, EphA4 could regulate branching by either repulsive or attractive interactions or possibly both (Fig. 8). If the signal were repulsive, then EphA4 in the environment might repel the growth of any new branches from the axon. Alternatively, the signal to the axon from EphA4 might be to remain fasciculated and prevent branching *per se*. It is also possible that axonal EphA4 could contribute to the process: EphA4–ephrin signaling could occur between the CST axons to stimulate fasciculation. CST axons are highly fasciculated during development, and a correlation between defasciculation and increased branching has already been established (34), specifically in the CST (18, 35). Further *in vivo* studies will be required to distinguish the roles of axonal and environmental EphA4 in CST development, such as targeting expression of dominant-negative forms of EphA4 in cortical neurons to block EphA4 function on CST axons.

EphA4 can interact with a range of different ephrin ligands, and previous studies have implicated ephrinB3 as the barrier that prevents EphA4-positive axons from recrossing the midline (10). Our studies of ephrinB3 are consistent with these findings and show clear expression of ephrinB3 on the midline of the spinal cord in postnatal animals. We find no evidence for ephrinB3 expression in the region of the CST. However, the differential expression of ephrinA5 across the motor cortex and within the DF is consistent with restricted expression on hindlimb CST axons and suggests interaction with EphA4 in CST guidance. The down-regulation of ephrinA5 in hindlimb motor cortex at the time of hindlimb branching in the cord is also consistent with a loss of EphA4–ephrinA5 interactions, thereby permitting branching of this subpopulation of axons (Fig. 8). An extensive analysis of ephrinA5 function (e.g., analysis of ephrinA5 knockout mice) in CST development will be required to verify its role, which is beyond the scope of the present study.

It is also possible that other unidentified ephrin ligands may contribute to EphA4-mediated regulation of topography in the CST. For example, EphA4 may mask coexpressed ephrins (36). To look for ephrins that may be masked by EphA4, we incubated sections of spinal cord from *EphA4*$^{-/-}$ mice with EphA4–Fc. Our preliminary observations suggested greater reactivity in the DF in the region of the CST from the *EphA4*$^{-/-}$ mice compared with control mice. EphrinA5 showed a similar increase in immunoreactivity in sections from *EphA4*$^{-/-}$ mice compared with control mice (data not shown), suggesting that its presence is partially masked by EphA4 in control mice. These preliminary observations are consistent with EphA4–ephrinA5 interactions being involved in CST guidance.

Materials and Methods

Anterograde Tracing. Multiple injections of 10% BDA (Molecular Probes, Eugene, OR) were administered to developing P1 anterior cortex or fore- or hindlimb aspects of the motor cortex (13, 37, 38) of anesthetized *EphA4*$^{-/-}$ and *EphA4*$^{+/-}$ pups (7). *EphA4*$^{+/-}$ mice do not display any CST abnormalities and were therefore selected as littermate controls (7). At either P5 or P7, pups were transcardially perfused with PBS and then 4% paraformaldehyde, postfixed for 2 h at 4°C in the same fixative, and cryoprotected in 30% sucrose-PBS for 48 h at 4°C before being rapidly frozen in OCT compound (Sakura, Torrence, CA). Serial cryostat coronal brain sections (100 μm) and horizontal or sagittal sections of the cervical spinal cord (20 and 50 μm) were collected onto 0.1% chromalum/1% gelatin-coated slides and incubated in Alexa Fluor 594-streptavidin (Molecular Probes) to visualize BDA. For labeling of fore- and hindlimb motor cortex, any animals with injection sites outside the specified area (for forelimb, within 3.4 mm from the rostral tip of the brain at the genu of the corpus callosum; for hindlimb, caudal to the beginning of the hippocampal commissure 5.7 mm from the rostral tip of the brain) or deeper than layer 6 of the cortical lamellae were not included for analysis. Every spinal cord section containing axonal projections in the DF from the layer 5 pyramidal cells of the motor cortex was analyzed; all labeled axons longer than 300 μm were counted, the trajectory of each exiting axon was ascertained, and the number of any branch points was recorded. Branch points were verified at $\times$100 magnification to ensure that they were true branches, and not two axons traveling within close proximity. A minimum of 150 axons were counted for each animal, and at least five animals of each age and genotype were assessed. To determine numbers of CST axons that reached the lumbar spinal cord, serial horizontal sections extending from cervical to lumbar enlargements were taken from P7 mice that had been injected with BDA in hindlimb motor cortex. The number of labeled axons present at the lumbar end of these sections was determined and expressed as a percentage of the number of labeled axons at the cervical end. Significance was determined by using Mann–Whitney analysis.

Immunohistochemistry. C57BL/6 neonatal brains and spinal cords (P0, P2, P5, and P11; $n = 5$ for each age) were either prepared as described above or frozen unfixed. Transverse cryosections (20 μm) were collected, and unfixed tissue was fixed for 5 min in ice-cold methanol, rinsed in PBS, and allowed to dry. Tissue was incubated in the appropriate blocking solution, followed by overnight incubation at room temperature in primary antibodies directed toward EphA4 (1:1,000; kindly donated by David Wilkinson, National Institute for Medical Research, Mill Hill, U.K.), ephrinA1 or -A2 (1:100; Santa Cruz Biotechnology, Santa Cruz, CA), ephrinA5 or -B3 (1:15; R & D Biosystems, Minneapolis, MN), and PSA-NCAM or NeuN (1:200 and 1:1,000; Chemicon International, Temecula, CA). Primary antibodies were visualized with the appropriate Alexa Fluor-coupled secondary antibodies (1:400; Molecular Probes). Methanol-fixed tissue was used for single labeling with EphA4 and ephrinA1 antibodies; all other immunohistochemistry was conducted by using paraformaldehyde-fixed tissue. Omission of all primary antibodies showed minimal nonspecific immunoreactivity.

For quantitative analysis of EphA4 immunoreactivity, tissue was collected from five animals at each age (from the same litter, where possible) and processed concurrently. For EphA4 and PSA-NCAM immunoreactivity in the DF, images were collected by using identical capture settings with an MRC 1024 confocal scanning laser microscope (Bio-Rad, Sydney, Australia). Grayscale images were merged by using Photoshop (Adobe, San Jose, CA), and an AnalySIS software package (Soft Imaging Systems, Münster, Germany) was used to create a binary mask to isolate any remaining green-only pixels. Using the EphA4 grayscale image, the number and intensity of these pixels was determined. Significance was determined by using Student's t test.

***In Vitro* Assay.** P3 C57BL/6 fore- and hindlimb motor cortices were dissected, and the middle third of the cortex, which predominantly contains layers 5 and 6 at this age, was isolated (Fig. 7) and dissociated with 0.25% trypsin. Cells were plated at low density (2×10^4 cells per well) in eight-well chamber slides

onto confluent monolayers of 293T cells that had been transfected 48 h previously with an EphA4 expression plasmid containing the murine EphA4 gene cloned into a pCI-neo vector (Promega, Madison, WI) or with a pBKCMV plasmid (Promega) by using Effectene transfection reagent (Qiagen, Valencia, CA). Cultures were grown in DMEM supplemented with FCS (10%), penicillin (100 units/ml), and streptomycin (100 μg/ml) for 24 h and fixed with 4% paraformaldehyde and then ice-cold methanol. After fixation, all slides were washed in PBS and labeled with antibodies for β-III tubulin (1:500; Covance, Richmond, CA) to identify neurites, EphA4 (1:100; Santa Cruz Biotechnology) to verify transfection, and the nuclear counterstain DAPI (Molecular Probes) to ascertain confluence. Antibody labeling was visualized with the appropriate fluorescent secondary antibodies (1:400; Molecular Probes). Control 293T cells transfected with the pBKCMV plasmid did not show any immunoreactivity for EphA4, which indicated no endogenous EphA4 expression by these cells (data not shown). At least 100 neurons with neurites in direct contact with EphA4-positive 293T cells from at least four separate wells in each condition were imaged by using Image-pro plus (Media Cybernetics, Silver Spring, MD). The number of primary neurites (neurites emanating from the cell body), length of the longest primary neurite, total primary neurite length, and number of branches were recorded. Only neurons that were not in contact with other neurons were included for analysis. Experiments were repeated at least twice, and ANOVA statistical analysis was performed to determine significance. All procedures were approved by the University of Melbourne Animal Ethics Committee and conducted in accordance with the relevant guidelines and regulations.

We thank Elizabeth Bateman and Johan Holmberg for help with ephrinA5 and Andrew Boyd (Queensland Institute of Medical Research, Brisbane, Queensland, Australia) and Mirella Dottori (Monash University, Clayton, Victoria, Australia) for use of the EphA4 mice. This work was supported by University of Melbourne and the National Health and Medical Research Council of Australia.

1. Kuang RZ, Merline M, Kalil K (1994) *Development (Cambridge, UK)* 120:1937–1947.
2. Joosten EA, van der Ven PF, Hooiveld MH, ten Donkelaar HJ (1991) *Neurosci Lett* 128:25–28.
3. Joosten EA, Gispen WH, Bar PR (1994) *Neuroscience* 59:33–41.
4. Kuang RZ, Kalil K (1994) *J Comp Neurol* 344:270–282.
5. Wilkinson DG (2001) *Nat Rev Neurosci* 2:155–164.
6. Kullander K, Mather NK, Diella F, Dottori M, Boyd AW, Klein R (2001) *Neuron* 29:73–84.
7. Dottori M, Hartley L, Galea M, Paxinos G, Polizzotto M, Kilpatrick T, Bartlett PF, Murphy M, Kontgen F, Boyd AW (1998) *Proc Natl Acad Sci USA* 95:13248–13253.
8. Coonan JR, Greferath U, Messenger J, Hartley L, Murphy M, Boyd AW, Dottori M, Galea MP, Bartlett PF (2001) *J Comp Neurol* 436:248–262.
9. Kullander K, Butt SJ, Lebret JM, Lundfald L, Restrepo CE, Rydstrom A, Klein R, Kiehn O (2003) *Science* 200:1889–1892.
10. Kullander K, Croll SD, Zimmer M, Pan L, McClain J, Hughes V, Zabski S, DeChiara TM, Klein R, Yancopoulos GD, Gale NW (2001) *Genes Dev* 15:877–888.
11. Gianino S, Stein SA, Li H, Lu X, Biesiada E, Ulas J, Xu XM (1999) *Brain Res Dev Brain Res* 112:189–204.
12. O'Leary DD, Bicknese AR, De Carlos JA, Heffner CD, Koester SE, Kutka LJ, Terashima T (1990) *Cold Spring Harbor Symp Quant Biol* 55:453–468.
13. Schreyer DJ, Jones EH (1988) *Brain Res* 466:89–101.
14. Akintunde A, Buxton DF (1992) *Brain Res* 575:86–92.
15. Chung KS, Coggeshall RE (1987) *J Neurosci* 7:972–977.
16. Yokoyama N, Romero MI, Cowan CA, Galvan P, Helmbacher F, Charnay P, Parada LF, Henkemeyer M (2001) *Neuron* 29:85–97.
17. Joosten EA, Reshilov LN, Gispen WH, Bar PR (1996) *Brain Res Dev Brain Res* 94:99–105.
18. Daston MM, Bastmeyer M, Rutishauser U, O'Leary DD (1996) *J Neurosci* 16:5488–5497.
19. Goldshmit Y, Galea M, Wise G, Bartlett P, Turnley A (2004) *J Neurosci* 24:10064–10073.
20. Flanagan JG, Vanderhaeghen P (1998) *Annu Rev Neurosci* 21:309–345.
21. Menzel P, Valencia F, Godement P, Dodelet VC, Pasquale EB (2001) *Dev Biol* 230:74–88.
22. Flanagan JG (2000) *Curr Biol* 10:R52–R53.
23. Sobieszczuk DF, Wilkinson DG (1999) *Curr Biol* 9:R469–R470.
24. O'Leary DD, Terashima T (1988) *Neuron* 1:901–910.
25. Liu Y, Shi J, Lu CC, Wang ZB, Lyuksyutova AI, Song X, Zou Y (2005) *Nat Neurosci* 8:1151–1159.
26. Schreyer DJ, Jones EG (1988) *Brain Res* 466:103–119.
27. Schreyer DJ, Jones EG (1982) *Neuroscience* 7:1837–1853.
28. Gorgels TG (1991) *J Comp Neurol* 306:95–116.
29. Kaufman MH (1992) *The Atlas of Mouse Development* (Academic, London).
30. Greferath U, Canty AJ, Messenger J, Murphy M (2002) *Mech Dev* 119(Suppl 1):S231–S238.
31. Cowan CA, Henkemeyer M (2002) *Trends Cell Biol* 12:339–346.
32. Caras IW (1997) *Cell Tissue Res* 290:261–264.
33. Eberhart J, Barr J, O'Connell S, Flagg A, Swartz ME, Cramer KS, Tosney KW, Pasquale EB, Krull CE (2004) *J Neurosci* 24:1070–1078.
34. Yeo S, Miyashita T, Fricke C, Little M, Yamada T, Kuwada J, Huh T, Chien C, Okamoto H (2004) *Mech Dev* 121:315–324.
35. Landmesser L, Dahm L, Tang JC, Rutishauser U (1990) *Neuron* 4:655–667.
36. Helmbacher F, Schneider-Maunoury S, Topilko P, Tiret L, Charnay P (2000) *Development (Cambridge, UK)* 127:3313–3324.
37. Joosten EA, Gribnau AA, Dederen PJ (1987) *Brain Res* 433:121–130.
38. Paxinos G, Franklin KBJ (2001) *The Mouse Brain in Stereotaxic Coordinates* (Academic, San Diego).